The decagonal plane-wave model for 2D and 3D quasicrystals

1994 J. Phys.: Condens. Matter 6 6197

(http://iopscience.iop.org/0953-8984/6/31/019)

J. Phys.: Condens. Matter 6 (1994) 6197–6210. Printed in the UK

The decagonal plane-wave model for 2D and 3D quasicrystals

R F Sabiryanov and S K Bose
Department of Physics, Brock University, St Catharines, Ontario, Canada L2S 3A1

Received 22 March 1994, in final form 10 May 1994

Abstract. We examine the free electron model for some rational approximants of 2D quasicrystals and quasi-lattices that exhibit quasiperiodicity in (x, y) planes and periodicity along the z-direction. Our study is based on a scattering potential with ten symmetrically oriented plane-wave components in the (k_x, k_y) plane for the 2D case, and two additional plane-wave components in directions perpendicular to the plane for the 3D case. We calculate the band structure and the density of states for the rational approximants and examine the formation of a gap or a pseudogap in such systems. The relevance of this study to the stability and electrical conduction property of decagonal quasicrystals is discussed.

1. Introduction

The present study was inspired by recent articles of Carlsson [1, 2], which examined the electronic density of states (DOS) for a model one-electron potential with twelve symmetrically oriented plane-wave components. Calculations based on this icosahedral plane-wave model reveal topological band structure differences that allow an icosahedral quasicrystal to have a gap in the DOS, while an analogous simple monoatomic BCC structure cannot. The issue of pseudogap formation in nearly free electron materials with icosahedral symmetry had previously been explored [3–5] via a two-plane-wave analysis based on the (pseudo-) Jones zone approach. The (pseudo-) Jones zone is the region in reciprocal space bounded by the perpendicular bisectors of the vectors joining the origin to the dominant scattering vectors, as obtained, for example, from diffraction experiments. It is believed that in these materials the Fermi wave vector lies on the (pseudo-) Jones zone boundary, and the origin of the pseudogap is a Hume-Rothery-like Fermi surface–(pseudo-)Jones zone boundary (FS–JZB) interaction. The pseudogap at the Fermi level lowers the electronic energy and is deemed to be an important factor in stabilizing the icosahedral phase. This is reminiscent of the Nagel–Tauc [6] criterion for the stability of metallic glasses. Elaborate and reliable electronic structure calculations for both icosahedral quasicrystals and their crystalline approximants [7, 8] reveal the existence of a pseudogap in the DOS at the Fermi level. The existence of pseudogap is also supported by conductivity, specific heat, and photoemission experiments [9] on icosahedral quasicrystals. In systems like AlMnSi, both the icosahedral quasicrystal phase (i-AlMnSi) and its close crystalline approximant (α-AlMnSi) [10] show evidence of a pseudogap. This is inferred from specific heat, semimetallic conductivity and other similar anomalous transport properties exhibited by both phases [9].

The icosahedral plane-wave analysis presented in [1, 2] has prompted us to carry out a similar study for systems which exhibit quasiperiodicity in (x, y) planes and periodicity along the z-direction. Decagonal quasicrystals, which exist in thermodynamically stable

0953-8984/94/316197+14$19.50

phases [11, 12], belong to this category. Measurements of the optical conductivities of decagonal quasicrystals [13] and an analysis based on a comparison with similar measurements on icosahedral systems indicate the possibility of significant differences in the electronic structure of these two classes of quasicrystals. The present study is intended to shed some light on this issue. We have carried out our investigation in two steps. First we examine the 2D quasiperiodic case via a model one-electron potential with ten plane-wave components with the wave vectors symmetrically arranged in a plane. This is a 2D analogue of the 3D icosahedral case studied by Carlsson [1, 2], and can be called the decagonal plane-wave model. We study the band structure and the DOS for various rational approximants and study the limiting behaviour for increasing order of the Fibonacci approximation (p/q) to the golden mean, τ. Next we consider the 3D case by adding two more plane-wave components to the potential in directions perpendicular to the plane, the direction of periodicity. The results for the band structure and the DOS for these 2D and the 3D cases are presented in section 2 of this paper. In section 3 we present a (pseudo-) Jones zone analysis of the gap formation and the states near the gap. In section 4 we discuss the relevance of our study to the properties of decagonal quasicrystals. In section 5 we summarize our results and present our conclusions. Our calculations are strictly for some low-order rational approximants of the 2D and 3D (decagonal) quasicrystals. The comments made for the exact quasicrystalline phases are based on observation of certain tendencies in these approximants.

2. Electronic structure for the decagonal plane-wave model

For the 2D quasicrystal the one-electron potential proposed by Carlsson [1, 2] can be written as

$$V(\boldsymbol{r}) = V_0 \sum_j \left(e^{i\boldsymbol{Q}_j\cdot\boldsymbol{r}} + e^{-i\boldsymbol{Q}_j\cdot\boldsymbol{r}}\right) \tag{1}$$

where $\boldsymbol{Q}_j$ are five symmetrically oriented vectors in the plane (figure 1), each having the same magnitude Q_0. V_0, chosen to be a positive constant, determines the strength of the scattering potential and the magnitude of the gap. Equation (1) represents a simplified form of the potential seen by the electron in an actual 2D quasicrystal, since the structure factor has peaks at many wave vectors (of different magnitudes)—in fact, an infinite number of them. Equation (1) can be extended to include other wave vectors, bearing quasiperiodic ratios to Q_0. We suppose that the vectors chosen in (1) are the strongest scattering vectors, i.e., with the largest magnitude of V_0. The effect of this simplification is expected to be weak as far as DOS properties are concerned. Localization properties of the wavefunctions, not addressed to in the present paper may, however, depend crucially on how many wave vectors are retained in the Fourier representation of $V(\boldsymbol{r})$. The magnitude Q_0 of the scattering vectors determines the location, E_g, of the gap in the DOS via $E_g = (\hbar^2/2m)(Q_0/2)^2$. For the 2D quasicrystal the vectors $\boldsymbol{Q}_i$ can be written as

$$\begin{aligned} \boldsymbol{Q}_2 &= Q_0\{(1+\tau^2)/2,\ 1/(2\tau)\} & \boldsymbol{Q}_5 &= Q_0\{-(1+\tau^2)/2,\ 1/(2\tau)\} \\ \boldsymbol{Q}_3 &= Q_0\{(1+\tau^2)/2\tau,\ -\tau/2\} & \boldsymbol{Q}_4 &= Q_0\{-(1+\tau^2)/2\tau,\ -\tau/2\} \end{aligned} \tag{2}$$

for the x- and y-axes as shown in figure 1. Q_1 can be determined from $\sum Q_i = 0$. To study the rational approximants of the 2D quasicrystal, we replace the golden mean, τ, by its Fibonacci approximant, p/q, with the corresponding vectors Q_i given by

$$\begin{aligned} Q_2 &= Q_0'\{p(p^2+q^2)^{1/2},\ q^2\} \qquad & Q_5 &= Q_0'\{-p(p^2+q^2)^{1/2},\ q^2\} \\ Q_3 &= Q_0'\{q(p^2+q^2)^{1/2},\ -p^2\} \qquad & Q_4 &= Q_0'\{-q(p^2+q^2)^{1/2},\ -p^2\} \end{aligned} \tag{3}$$

where $Q_0' = Q_0/(p^4 + p^2q^2 + q^4)^{1/2}$. We calculate the band structure and the DOS for a series of rational approximants to the 2D quasicrystal. A natural way to choose the periodic approximant is to consider a rectangular unit cell with basis vectors a and b as shown in figure 1. This is the smallest unit cell that allows interaction between the states at various reciprocal lattice vectors via all the vectors Q_i, thus using the full symmetry of the potential $V(r)$. This choice gives in the limit $p, q \to \infty$, $p/q \to \tau$, $a/b = (1+\tau^2)^{1/2}/2$ (figure 1). Thus for the p/q approximant we take

$$a = Q_0'\{(p^2+q^2)^{1/2},\ 0\} \qquad b = Q_0'\{0,\ 2q\}. \tag{4}$$

The unit cell for the 1/1 approximant, with the symmetry points, is shown with solid lines in figure 2. The significance of the dashed lines is to show the connection with a distorted hexagonal symmetry to be discussed at a later stage.

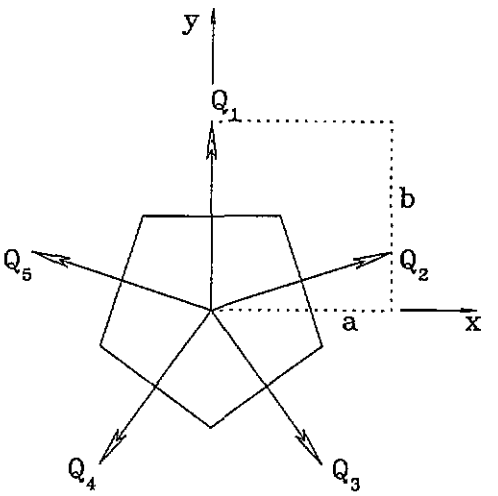

Figure 1. Scattering vectors (Q_i, $i = 1, \ldots 5$) (equations (1) and (2)) and the corresponding pentagonal (pseudo-) Jones zone. The (pseudo-) Jones zone with all the ten vectors in equation (1) is decagonal. The unit cell (a, b) used in the calculation is indicated with dotted lines.

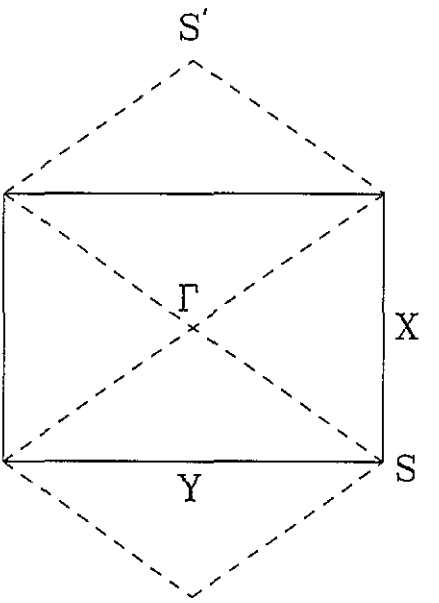

Figure 2. Unit cell for the 1/1 approximant with the symmetry points indicated by Γ, S, X and Y. The dashed lines indicate a distorted hexagonal symmetry (see discussion in the text).

For the 3D case, i.e. 3D lattices quasiperiodic in a plane and periodic in the perpendicular direction, we modify the decagonal plane-wave model given by (1) by adding two plane waves, one in each direction perpendicular to the quasiperiodic plane. The purpose is to be able to comment, based on some rational approximant calculations, on the properties of decagonal quasicrystals. The magnitude of these vectors is taken to be Q_0. The unit cell used in the 3D calculation is, thus, constituted by the vectors a, b, and c, where c is a vector of magnitude Q_0 in the z-direction. This choice is consistent with the structure of the decagonal phase of the Al–Mn quasicrystal discussed by Daulton *et al* [11]. It is also based on the observation [14] that the decagonal quasicrystal possesses a screw axis, very much like the HCP structure, resulting in effective obliteration of the odd Bragg planes at $(2n+1)\pi/c$ (c = separation between the planes) in the z-direction. Steurer and co-workers have determined and discussed the structures of decagonal quasicrystals Al–Cu–Co [15], Al–Mn [16], and Al–Ni–Co [17]. Burkov [18] has presented a structural model for the decagonal Al–Cu–Co, which is a reformulation and extension of Steurer's model [15]. In this model of decagonal Al–Cu–Co the obliteration of the odd Bragg planes in the z-direction has the effect of putting the effective first Brillouin zone boundary (i.e. JZB) at the same distance from the Γ point in the z-direction as in the quasiperiodic plane. Our choice of the magnitude of c ($= Q_0$) is in consistence with this result. However, as we will see the choice of the magnitude of the vectors in the z-direction in the Fourier components of $V(r)$ is not crucial to the basic important features of our results.

The results for the band structure for the 2D case for 1/1, 2/1 and 3/2 rational approximants are shown in figure 3 (top to bottom). The corresponding DOSs are shown in figure 4, presented as the ratio of the DOS to the free-electron DOS for the empty lattice. Even for the 1/1 approximant a gap appears in the DOS for $V_0 \sim 0.15$ Ryd ($\hbar^2/2m$ set to unity). This is not surprising, since each point on the first Brillouin zone boundary has only one equivalent point, eliminating the possibility of degeneracy. The results shown in figures 3 and 4 are obtained using $V_0 = 0.2$ Ryd and a kinetic energy cut-off at 2.57 Ryd. The cut-off was gradually reduced starting from a high value ($\sim$ 16 Ryd) so the calculation could be carried out with a relatively small number of plane waves (reciprocal lattice vectors). The stability of the results with respect to this cut-off was insured. The 2D 1/1 approximant considered by us is almost like a planar cut of the 3/2 approximant in the icosahedral plane-wave model considered by Carlsson [1,2]. The size of the unit cell in real space grows faster (as p^2) in our case than in the icosahedral plane-wave model of Carlsson [1,2] (as p). Thus the size of the Brillouin zone and the length of the reciprocal lattice vectors decrease rapidly with the increasing order of the approximant, requiring a fast increasing number of reciprocal lattice vectors to cover the same energy range. The 5/3 approximant would have needed more than 2000 plane waves in our calculation, forcing us to stop at the 3/2 level. However, it seems that higher-order approximants will not yield any new information except the saturation value of the gap width. The difference between the gap widths for the 2/1 and 3/2 rational approximants is very small ($\sim$3%), i.e., the gap width is close to its saturation value (V_0) already at the 3/2 level.

The band structure for the 3D case is shown in figure 5 for the 2/1 approximant. The bands in the (k_x, k_y) (quasiperiodic) plane are very similar to the 2D case. An examination of the band structure for the three approximants (not shown here) reveals that the bands in the (k_x, k_y) plane become flatter with increasing order of the approximant. The bands in the periodic k_z direction are the usual parabolic free-electron-like bands. These parabolic bands modify the DOS, changing the gap in the 2D case into a quasi-gap, i.e., just a minimum in the DOS. The DOSs obtained for the 1/1, 2/1, and 3/2 approximants are shown in figure 6, presented as the ratio of DOS and that at the pseudogap region, $E_g = 0.6$ Ryd. It is clear

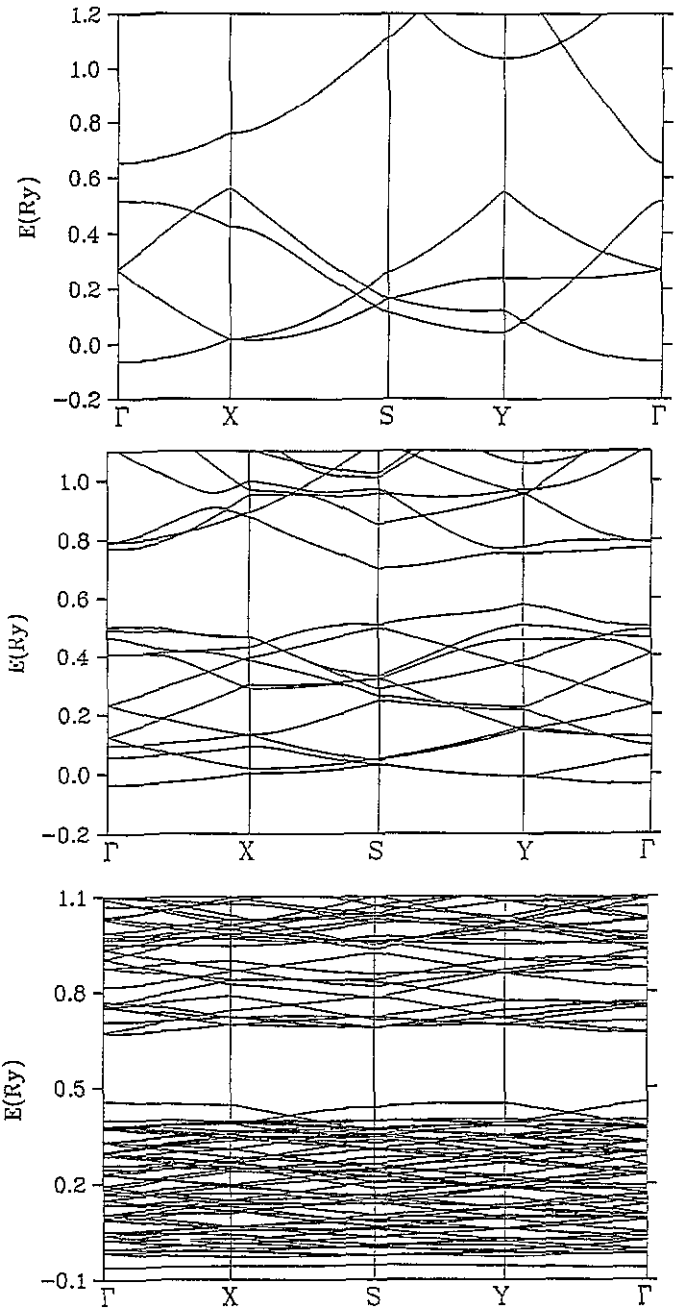

Figure 3. (top to bottom) Band structures for the 1/1, 2/1, and 3/2 approximants, respectively, for the 2D case.

that the periodicity in the z-direction removes the gap in the DOS, and changes it, at best, to a minimum in the DOS. The depth of this quasi-gap is dependent on the curvature of the parabolic bands in the k_z direction, i.e., to the choice of the vector c for the unit cell. As stated earlier our choice is guided naturally by the Steurer [15] and Burkov models [18] of the decagonal Al–Cu–Co quasicrystal. Note that the DOSs in figure 6 show wiggles due to

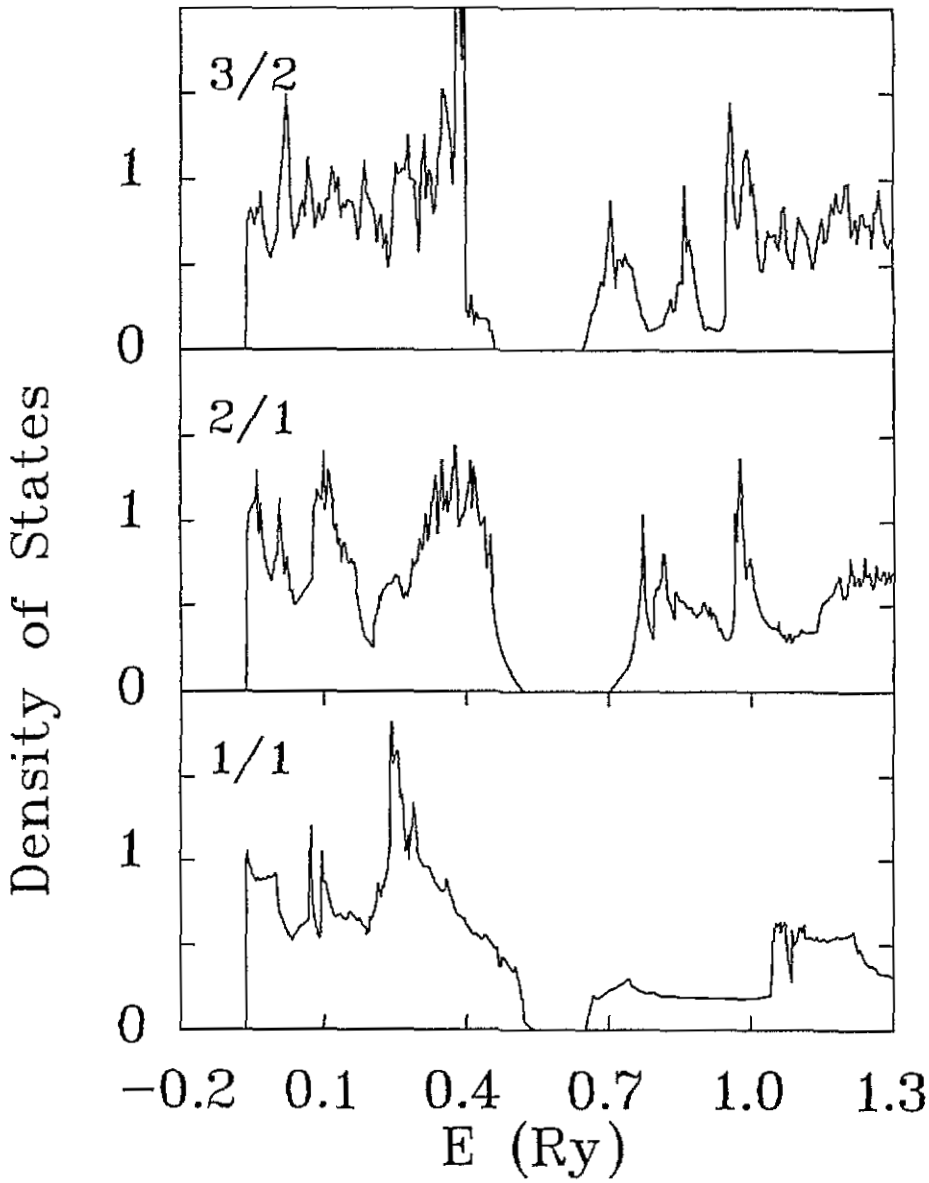

Figure 4. DOS for the 1/1, 2/1, and 3/2 approximants in 2D, presented as the ratio of the DOS and the free electron DOS for the empty lattice.

a finite number of k-points used in the calculation. A smoother DOS could be obtained by using more k-points or by using an energy-dependent matrix element as done by Carlsson [1, 2] (see equation (3) of [2]).

3. Gap formation and states near the gap edges

The following discussion is very similar to the (pseudo-) Jones zone analysis presented by

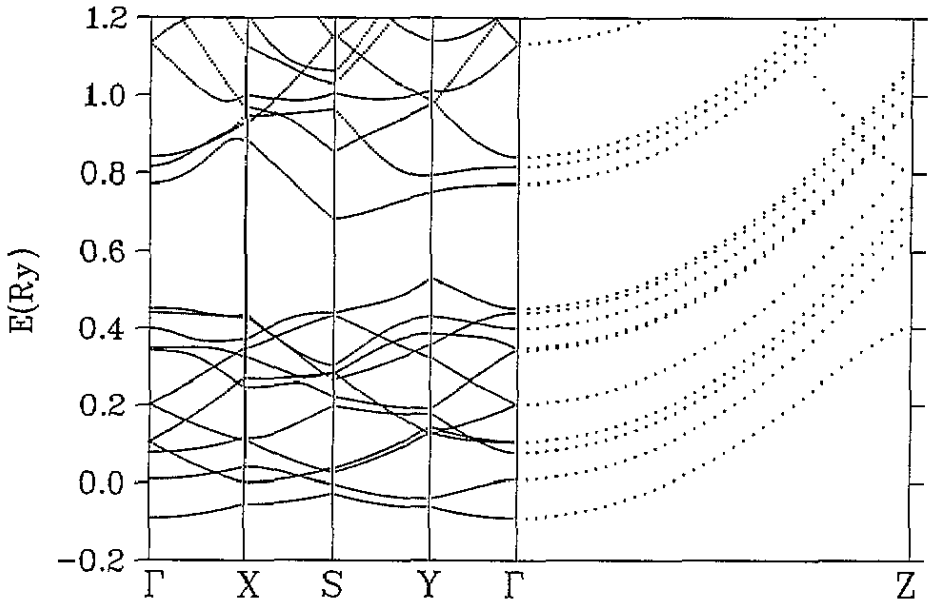

Figure 5. Band structure for the 2/1 approximant for the 3D case.

Carlsson [1,2] in connection with gap formation in icosahedral quasicrystals. We examine the energy eigenvalues at the boundary of the (pseudo-) Jones zone (in the crystalline case, first Brillouin zone) for the 2D case. To start with, let us consider the first Brillouin zone of a hexagonal lattice, shown in figure 7(a). The corner points belong to two classes of equivalent points, H_1 and H_2. Equivalent points belonging to the same class are shown joined by dotted lines. Because of the threefold degeneracy we need a three-wave analysis at the corner points. This analysis gives a non-degenerate energy level, $E_0^{\mathrm{H}} + 2V_0$, and a doubly degenerate energy level, $E_0^{\mathrm{H}} - V_0$, where E_0^{H} is the energy of the unperturbed plane wave at the corner point. For $V_0 > 0$ the lower level is thus twofold degenerate even in the presence of the perturbing crystalline potential. The edge-centre points L have only one equivalent point, and a two-wave analysis yields eigenvalues $E_0^{\mathrm{L}} \pm V_0$. In figure 8(a) we sketch the bands along the symmetry direction HL, showing that there cannot be any gap in the DOS. In figure 7(b) we show the first Brillouin zone of a square lattice. The four corner points H are equivalent and a four-plane-wave analysis yields a non-degenerate eigenvalue $E_0^{\mathrm{H}} - 3V_0$, and a triply degenerate eigenvalue $E_0^{\mathrm{H}} + V_0$. At the edge-centre point N a two-plane-wave analysis is valid and yields eigenvalues $E_0^{\mathrm{N}} \pm V_0$. The corresponding bands, sketched in figure 8(b), show that there is a gap in the DOS of magnitude $2V_0$. As shown in the previous section, the fivefold-symmetric (pseudo-) Jones zone (figure 1), with no equivalent points on the zone boundary, admits of an energy gap. The width of the gap is lowest for the 1/1 approximant, with a rectangular Brillouin zone (twofold symmetry) and increases as the order of the approximant increases. For the twofold symmetry the gap, V_0' (dependent on the ratio a/b), is less than $2V_0$, while for tenfold (fivefold) symmetry the gap is greater than V_0', but less than $2V_0$. Note that in the case of the 1/1 approximant the rectangular unit cell in the reciprocal space (figure 2) can be seen as a distorted square, but the unit cell can also be chosen as the parallelogram with vertices at S′, Γ and S. This unit cell can be seen as a distorted version of a similar unit cell for the hexagonal lattice ($H_2\Gamma H_2H_1$ in figure 7(a)). Thus the 1/1 approximant has a gap of width intermediate

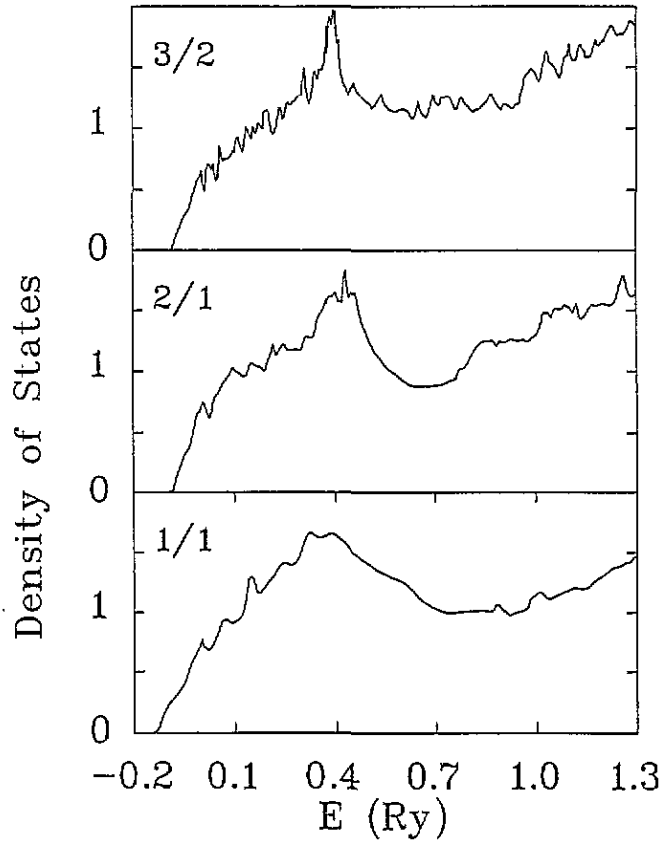

Figure 6. DOS for the 1/1, 2/1, and 3/2 approximants for the 3D case, presented as the ratio of the DOS and the DOS at 0.6 Ryd.

between $2V_0$ (square lattice) and 0 (hexagonal lattice).

For the decagonal (pentagonal) symmetry, there are two mechanisms that determine the changes near the gap edges with the increasing order of the approximant. The dominant effect is due to a change in the ratio a/b, which causes a change in the location of the band edges. This change is stronger in the beginning, i.e., for lower-order approximants. With increasing order (p/q) the a/b ratio, $(p^2+q^2)^{1/2}/2q$, oscillates about the limit $(1+\tau^2)^{1/2}/2$ with gradually diminishing amplitude. The change in the a/b ratio with the order also affects the shape of the DOS near the gap edges via a change in the reciprocal lattice vectors that contribute to states near the gap edges. The change in the gap width is thus a combination of a weak change in the shape of DOS near the gap edges overlapping a dominant change due to the movement of the gap edges. This is clear from an inspection of the DOSs shown in figure 4.

It is possible to understand the gap edge states via a simplified analysis. To illustrate this we consider the 3/2 approximant. It is clear from the band structure in figure 3(c) that the bands near the Γ point play the dominant role in determining the DOS at the bottom gap edge. The reciprocal lattice vectors, K_s, contributing to the eigenstates in this region satisfy the relation $K_s = Q_0/2$. In terms of basis vectors a and b, the vectors Q_i are given by

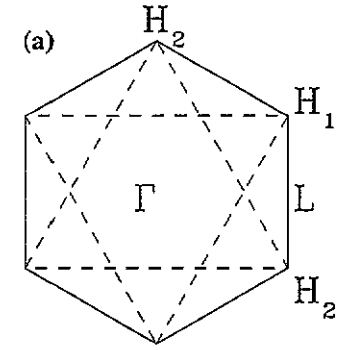

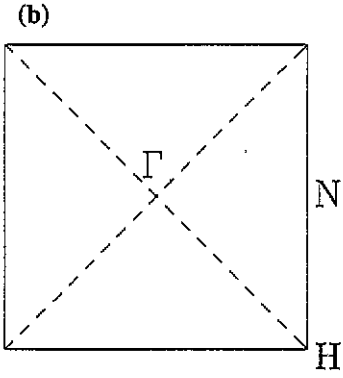

Figure 7. Brillouin zones for (a) hexagonal, (b) square lattice. The equivalent points are joined by dotted lines.

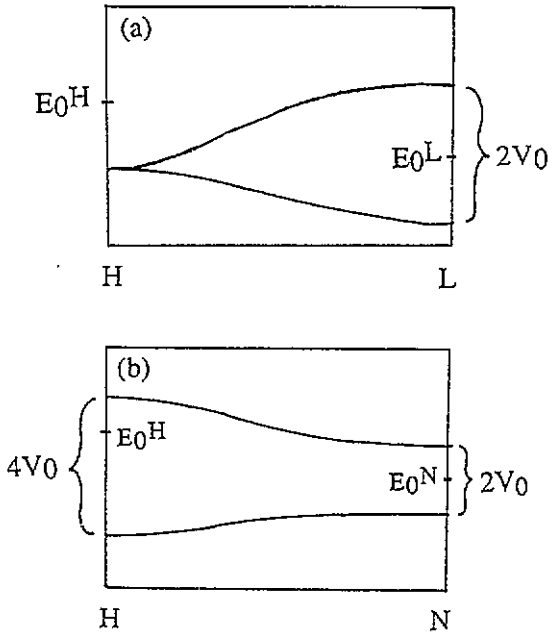

Figure 8. Schematic of the band structure in the symmetry directions (a) HL (hexagonal symmetry), and (b) HN (fourfold symmetry), corresponding to the Brillouin zones shown in figures 7(a) and 7(b), respectively.

$$Q_2 = Aa + Bb \qquad Q_3 = Ca + Db$$

with $A = 2pq$, $B = p^2$, $C = 2p^2$, $D = -q^2$. Q_4 and Q_5 can be obtained from Q_3 and Q_2 via the symmetry relation shown in figure 1 (and equation (2)). $\sum Q_i = 0$ yields $Q_1 = 2(-B + D)b$. For the 3/2 approximant there are a large number of reciprocal lattice vectors satisfying approximately the condition $K_s = Q_0/2$ (for example, the vectors (3, 6) (i.e., $K_s = 3a + 6b$); (9, 2); (1, 7); (7 0); (5, 4); (3, 5); (2, 6); (6, 3); (6, 1) etc). All these vectors lying in a shell around a circle of radius $Q_0/2$ have slightly different unperturbed energies. As p/q approaches τ, this shell becomes thinner and thinner. This is because for the vector $Q_i/2$, $p^2/2$ and $q^2/2$ should be chosen as the closest integers for odd p, q, and in the infinite limit the difference between these integers will vanish. Consider for the 3/2 approximant two unperturbed states (2, 6) and (6, 3), coupled via the Q_3 $(8a + 9b)$ component of the potential $V(r)$. The unperturbed state (6, 3) is coupled also to (6, 1) via Q_2 $(12a + 4b)$. There is no direct coupling between the states (2, 6) and (6, 1), but an indirect coupling mediated by (6, 3). However, we can create states

$$|\Psi_{26}\rangle = (1/2)\{|2, 6\rangle - |-2, 6\rangle - |2, -6\rangle + |-2, -6\rangle\}$$
$$|\Psi_{63}\rangle = (1/2)\{|6, 3\rangle - |-6, 3\rangle - |6, -3\rangle + |-6, -3\rangle\}$$

both of which are uncoupled from the state (6, 1), while the matrix element of the one-electron Hamiltonian between them is V_0. Thus the eigenvalues in the presence of the potential $V(r)$ can be obtained from the matrix

$$\begin{bmatrix} E_0^{2,6} & V_0 \\ V_0 & E_0^{6,3} \end{bmatrix}.$$

The eigenvalues in the presence of the potential $V(r)$ are thus further apart than the unperturbed energies. Similar analysis can be carried out for other sets of states such as {(3, 6); (9, 2); (1, 7)} or {(7, 0); (5, 4); (3, 5)}. All these unperturbed states with slightly different energies are spread further apart via the potential $V(r)$, giving rise to some structure in the DOS near the gap edges. In the infinite limit, when p/q has reached τ, the unperturbed energies merge, reducing somewhat the fine structure in the DOS near the gap edge.

Various features in the DOS are related to the shape and the arrangement of the bands, i.e., their deviation from the parabolic bands as a result of the interaction $V(r)$. In the absence of this interaction the DOS in the 2D case would have been a constant. In [1], the possibility of band-tailing in the gap region was suggested for the 3D icosahedral plane-wave model. With this in mind we look at the shape of the DOS at the gap edges for the 2D case, shown in figure 9. First of all we notice that V_0 must be strong enough to create a gap. Such strong potentials can cause significant deviation from the parabolic shape of the unperturbed bands, and we do see linear bands near various symmetry points. The linear bands give rise to linear DOS, whereas parabolic bands give constant DOS in 2D. The connection between the band shape and the shape of the DOS in the gap region can be seen by comparing the band structure of figure 3(top to bottom) with the DOS in figure 9. For the 1/1 approximant X and Y points (very close in energy) define the bottom of the gap. The linear bands in this region give rise to a linear DOS. The band at the Γ point, starting at a slightly lower energy, is parabolic and shifts the DOS by a constant. The top edge of the gap gets a contribution from the parabolic bands at the Γ point, with a constant DOS in this region. For the 2/1 approximant the top and bottom parts of the gap region get contribution from the linear bands near S and Y points, respectively, and the corresponding DOSs are linear. For the 3/2 approximant the bands at the top and bottom of the gap are a mixture of linear and parabolic parts. The corresponding DOS consists of linear parts, joined by constant shifts. The structure in the DOS near the bottom edge of the gap is due to a few bands that are separate from the rest of the bands at lower energy. Although all the preceding observations are trivial, the point here is that the shape of the DOS is easy to explain on the basis of the shape of the bands in our calculation and there is no indication of band-tailing. In 3D, linear bands give rise to parabolic DOS ($\sim E^2$) and parabolic bands give square-root DOS ($\sim E^{1/2}$). Since we have not performed the icosahedral model calculation, we cannot comment on whether the band-tailing suggested in [1] is due to linear bands giving E^2-like DOS.

Our analysis shows that if a free-electron-like 2D solid is to be stabilized via a Hume-Rothery-like mechanism, where the Fermi surface lies at the first Brillouin zone (or pseudo-Jones zone) boundary, then a square lattice is favoured over a hexagonal lattice as well as some lower-order approximants of 2D quasicrystals. From the observed closeness (or near saturation) in the gap width between the 2/1 and 3/2 approximants, we infer that the square lattice can be stable for a large enough V_0, but it may be difficult to realize such a structure experimentally because of competition from the crystalline structure (square lattice). Note that the issue of (non-existence of long-range positional order in

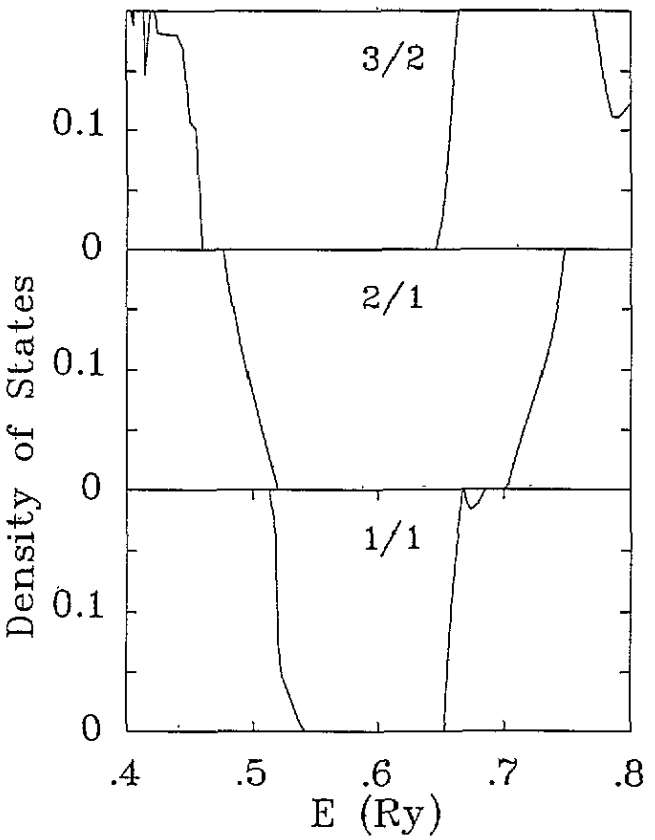

Figure 9. DOSS for the 2D approximants in the gap region.

2D, which is still an active area or research [19], is not the concern of this paper. We have compared electronic structures for 2D free-electron-like systems with potentials having certain symmetries, without any regard to how these symmetries might actually arise. A tight-binding analysis by Sire [20] shows that for a weak potential the crystalline phase is more stable than the quasicrystalline one in 2D, while the opposite situation is obtained by increasing the potential. Our results agrees with this result for weak potentials, while the tight-binding description of Sire [20] may well be more appropriate for systems that show significant deviation from free electron behaviour, i.e., systems with d electrons.

4. Application to the study of decagonal quasicrystals

The decagonal quasicrystals form a class of anisotropic materials with periodicity along their c-axis and quasiperiodic structure with tenfold symmetry in the plane perpendicular to the c-axis. Al–Cu–Co and Al–Ni–Co systems are examples of thermodynamically stable decagonal quasicrystals, while Al–Mn, Al–Fe and Al–Pd systems exist only in metastable decagonal phase [9]. Measurements of transport properties in single-grained decagonal quasicrystals show marked anisotropy [9, 13]. Electrical resistivity along the quasiperiodic plane can be 5–20 times higher than along the c-axis. There are reasons to believe that

the electrical conduction property of these systems is dominated by free-electron-like s–p states at the Fermi level. Self-consistent electronic structure calculations based on the LMTO (linear muffin-tin orbitals) [21] method for the Burkov model [18] of the decagonal Al–Cu–co quasicrystal, for various choices of the locations as well as concentrations of the transition metal atoms, Cu and Co, show [22] that s, p states and the d states have roughly equal weight at the Fermi level. The d-orbital-projected DOS at the Fermi level is approximately 50% of the total DOS. Since the mobility of the s, p states is, in general, several times higher than that of the d states [23], it is clear that the process of electrical conduction should be dictated by the free-electron-like s-p states at the Fermi level. The band structure in figure 5 shows that the flat bands in the quasiperiodic plane (suggesting high effective mass for the carriers in these states) can be responsible for the high in-plane electrical resistivity, while the parabolic free-electron-like bands in the periodic direction suggest low resistivity perpendicular to the plane. It seems that the band mechanism is adequate to explain the anisotropy in the electrical conduction, and no assumption regarding the criticality or the localization of the states at the Fermi level [24–26] is needed. This conclusion is in line with the assumption made by Burkov *et al* [27] in a theoretical study of the optical conductivity of icosahedral quasicrystals, i.e., the assumption that the conduction process is amenable to a k-space description. This assumption also underlies the study of the transport properties of icosahedral quasicrystals by Fujiwara [28]. It is valid for both icosahedral and decagonal quasicrystals.

Basov *et al* [13] have recently carried out measurements of optical and far-infrared conductivity of high-quality decagonal quasicrystals $Al_{65}Co_{17}Cu_{18}$ and $Al_{64}Co_{19}Cu_{15}Si_2$, and presented an analysis of their results based on a comparison with similar measurements on icosahedral quasicrystals. They find no evidence for a well-developed pseudogap at the Fermi level. Although neither this work nor that of Basov *et al* [13] provides a definitive clue to the (non-) existence of pseudogap in decagonal quasicrystals, our free electron model strongly suggests that the periodicity along the c-axis should suppress the gap to a large extent. Thus, the pseudogap in the decagonal phase, if at all present, should be much weaker than in the icosahedral phase. Note that this observation applies only to the free-electron-like states, while real quasicrystals, icosahedral and decagonal, have a large number of d electrons per atom. Rigorous calculations [22, 29] for the Burkov model [18] of the decagonal quasicrystals show that these d electrons play a crucial role in the stability of the quasicrystalline phase, even though their contribution to the conduction properties may not be dominant.

5. Summary and conclusions

Calculations based on the decagonal plane-wave model suggests that in 2D a quasicrystal with fivefold (tenfold) symmetry should exhibit an energy gap. This conclusion is based on our calculations of 1/1, 2/1, and 3/2 approximants. The width of the gap should be lower than that in case of fourfold symmetry (square lattice), but higher than that for twofold symmetry (rectangular lattice). 3D quasicrystals that exhibit decagonal symmetry in a plane but are periodic in the perpendicular direction should have no energy gap, but only a minimum in the DOS, because of the parabolic free-electron-like bands in the k_z direction. Thus the periodicity in the z-direction is detrimental to the formation of energy gap. For such quasicrystals that bands in the quasiperiodic (k_x, k_y) plane are much flatter than in the periodic k_z direction. Thus those decagonal 3D quasicrystals, where the electronic transport is dominated by free-electron-like states, should exhibit much larger resistivity

in the quasiperiodic plane than in the periodic direction. Finally, since the icosahedral plane-wave model [1, 2] for 3D quasicrystals exhibits an energy gap, while the decagonal plane-wave model does not, it is quite likely that in real 3D decagonal quasicrystals, such as Al–Cu–Co or Al–Ni–Co, the pseudogap at the Fermi level, if at all present, is much less pronounced than in similar (i.e., having roughly the same number of free and d electrons per atom) icosahedral quasicrystals. This, however, should not be interpreted as the decagonal quasicrystals being less stable, as a proper description of stability must address the role of the d electrons present in both icosahedral and decagonal quasicrystals. All the above conclusions are based on calculations for rational approximants.

Acknowledgments

Financial support for this work was provided by the Natural Sciences and Engineering Research Council of Canada.

References

[1] Carlsson A E 1993 *J. Non-Cryst. Solids* **153 & 154** 386
[2] Carlsson A E 1993 *Phys. Rev.* B **47** 2515
[3] Friedel J and Denoyer F 1987 *C. R. Acad. Sci., Paris* **305** 171
[4] Friedel J 1988 *Helv. Phys. Acta* **61** 538
[5] Smith A P and Ashcroft N W 1987 *Phys. Rev. Lett.* **59** 1365
[6] Nagel S R and Tauc J 1975 *Phys. Rev. Lett.* **35** 380
[7] Fujiwara T and Yokokawa T 1992 *Phys. Rev. Lett.* **66** 333
Fujiwara T 1989 *Phys. Rev.* B **40** 942
[8] Hafner J and Krajci M 1992 *Phys. Rev. Lett.* **68** 2321; 1992 *J. Non-Cryst. Solids* **150** 337
[9] Poon S J 1992 *Adv. Phys.* **41** 303
[10] Goldman A I and Kelton R F 1993 *Rev. Mod. Phys.* **65** 213
[11] Daulton T L and Kelton K F 1992 *Phil. Mag.* B **66** 37
Daulton T L, Kelton K F and Gibbons P C 1992 *Phil. Mag.* B **66** 311
[12] Grushko B 1992 *Phil. Mag. Lett.* **66** 151
[13] Basov D N, Timusk T, Bakarat F, Greedan J and Grushko B 1994 *Phys. Rev. Lett.* **72** 1937
[14] Lück R and Kek S 1993 *J. Non-Cryst. Solids* **153 & 154** 329
[15] Steurer W and Kuo K H 1990 *Acta Crystallogr.* B **46** 703
[16] Steurer W 1991 *J. Phys.: Condens. Matter* **3** 3397
[17] Steurer W, Haibach T, Zhang B, Kek S and Lück R 1993 *Acta Crystallogr.* B **49** 661
[18] Burkov S E 1993 *Phys. Rev.* B **47** 12325; 1991 *Phys. Rev. Lett.* **67** 614; 1992 *J. Physique* I **2** 695; 1992 *Physics and Chemistry of Finite Systems: From Clusters to Crystals (NATO ASI series, vol 374)* ed P Jena, S N Khanna and B K Rao (Dordrecht: Kluwer) pp 77–83
[19] Strandburg K J 1988 *Rev. Mod. Phys.* **60** 161 and references therein
[20] Sire C 1991 *J. Phys. A: Math. Gen.* **24** 5137
[21] Anderson O K, Jepsen O and Sob M 1987 *Electronic Structure and Its Applications (Springer Lecture Notes in Physics 283)* ed M Yussouff (Berlin: Springer) pp 1–57b and references therein
[22] Sabiryanov R F, Bose S K and Burkov S E 1994 *Phys. Rev.* B submitted
[23] Bose S K, Jepson O and Anderson O K 1993 *Phys. Rev.* B **48** 4265 and references therein
[24] Tsunetsugu H, Fujiwara T, Ueda K and Tokohiro T 1991 *Phys. Rev.* B **43** 8879; 1986 *J. Phys. Soc. Japan* **55** 1420
[25] Tsunetsugu H and Ueda K 1991 *Phys. Rev.* B **43** 8892
[26] Kitaev A Y 1987 *JETP Lett.* **487** 299
[27] Burkov S E, Timusk T and Ashcroft N W 1992 *J. Phys.: Condens. Matter* **4** 9447; 1993 *J. Non-Cryst. Solids* **153 & 154** 380; 1993 *Proc. 4th Int. Conf. on Quasicrystals (St Louis, MO, 1992)* ed K F Kelton, P C Gibbons and A I Goldman (Amsterdam: North-Holland)

[28] Fujiwara T 1993 *J. Non-Cryst. Solids* **156 & 158** 856; 1993 *Proc. 8th Int. Conf. on Liquid and Amorphous Metals (LAM8) (Wien, Austria, 1993)* ed J Hafner (Amsterdam: North-Holland)

[29] Trambly de Laissardiere G and Fujiwara T 1994 *8th Int. Conf. on Rapidly Quenched and Metastable Material (Sendai, 1993)*; *Mater. Sci. Eng.* A submitted